REPORT DOCUMENTATION PAGE

Form Approved
OMB No. 0704-0188

1. AGENCY USE ONLY *(Leave Blank)*	2. REPORT DATE	3. REPORT TYPE AND DATES COVERED
	January 1998	Final : 960201 to 980131

4. TITLE AND SUBTITLE
Deformation Behavior of Thin Lubricant Films at Elevated Pressure

5. FUNDING NUMBERS
Grant No.: N00014-96-1-0293

6. AUTHORS(S)
Scott Bair

7. PERFORMING ORGANIZATION NAME(S) AND ADDRESS(ES)
Scott Bair
Georgia Institute of Technology
School of Mechanical Enigneering
Atlanta, GA 30332-0405

8. PERFORMING ORGANIZATION REPORT NUMBER
Deliverable 2

9. SPONSORING/MONITORING AGENCY NAME(S) AND ADDRESS(ES)
Office of Naval Research, Ballston Centre Tower One, 800 North Quincy Street.
Arlington, VA 22217-5660

10. SPONSORING/MONITORING AGENCY REPORT NUMBER

11. SUPPLEMENTARY NOTES COR:

12a. DISTRIBUTION/AVAILABILITY STATEMENT
Approved For Public Release

12b. DISTRIBUTION CODE

13. ABSTRACT *(Maximum 200 words)*

If care is taken to avoid viscous heating, the results from rheometers may be used to generate empirical rate equations which are useful in modelling EHD traction. However, an analytical treatment of piezo-viscous liquids reveals the Reynolds equation adequately captures the mechanics of the piezo-viscous liquid only when the shear stress is much less than the reciprocal of the pressure viscosity coefficient. Otherwise the cross film pressure gradient cannot be neglected and secondary flows result.

14. SUBJECT TERMS
High -Pressure, Viscosity, Rheology, Elastohydrodynamics Shear Bands.

15. NUMBER OF PAGES
45

16. PRICE CODE

17. SECURITY CLASSIFICATION OF REPORT	18. SECURITY CLASSIFICATION OF THIS PAGE	19. SECURITY CLASSIFICATION OF ABSTRACT	20. LIMITATION OF ABSTRACT
Unclassified	Unclassified	Unclassified	Unlimited

DEFORMATION BEHAVIOR OF THIN LUBRICANT FILMS AT ELEVATED PRESSURE

January 1998

A Report to the Office of Naval Research
800 North Quincy Street
Arlington, VA 22217-5000

by Scott Bair
Principal Research Engineer
George W. Woodruff School of Mechanical Engineering
Georgia Institute of Technology

1. INTRODUCTION

1.1 CONSTITUTIVE BEHAVIOR

In the elastohydrodynamic (EHD) regime of lubrication, the rheology of the liquid lubricant is key to the generation of a protective film and the transfer of shear across concentrated contacts in many machine elements. It is now understood that small scale EHD plays a major role in the boundary lubrication of rough surfaces. Many high-pressure metal working operations share the pressure and kinematics of elastohydrodynamics. A complete solution of the EHD problem, however, requires a thorough knowledge of the lubricant constitutive behavior and the attending properties as functions of temperature and pressure. The Newtonian assumption alone is often inadequate, and the assumptions upon which the Reynolds equation is based must be re-examined.

Early investigations of high-pressure lubricant rheology addressed the small strain response. For small strains, viscous heating which plagues large strain measurements may be ignored. These measurements were both optical and acoustical, e.g. references [1] and [2] respectively, and provided linear viscoelastic properties. These techniques are experimentally convenient in requiring only optical or electrical paths through the high-pressure chamber. The linear viscoelastic response is, however, unable to account for any but the small slip traction in EHD.

Attention then turned to large strain investigations which could reveal non-linear behavior and successfully predict EHD traction [3]. The progress in this area has recently been significant in that a mechanism of apparent non-linearity (at least for low molecular weight liquids) has been shown to be a mechanically induced shear localization or shear

bands [4]. The constitutive behavior in the material surrounding the shear bands is apparently linear viscoelastic.

Fundamental to the generation of a film in concentrated contacts is the piezoviscous property of liquid lubricants - whereby even simple low molecular weight liquids at ambient temperature attain very great viscosities under pressure. Shear rheological investigations of non-Newtonian response of lubricants [5,6] have resorted to low temperatures to achieve the same level of viscosity. It is clear now, that high-pressure is essential to an accurate simulation. Liquids become considerably "stronger" under pressure. Peculiar to these atmospheric pressure studies was the observation of fracture. Eastwood and Harrison [5] observed the liquid in shear and reported cracking.

Early investigations of non-Newtonian lubricant response often studied polymer solutions. The blend of mineral base oil and polymeric viscosity index improver is representative of multi-grade motor oils. The capillary rheometer was useful for this purpose as it is very simply pressurized and although the shear stress cannot be large for this instrument, non-Newtonian flow occurs at relatively low stress for polymer solutions. The high-pressure capillary viscometer was developed to a high level by Jakobsen and Winer [7] who reported measurements to shear rates of $10^7 s^{-1}$, pressures to 600 MPa and time of shear as short as 4 μs. They reported Newtonian flow for liquid lubricant base stocks to a shear stress of 5 MPa.

1.2 REYNOLDS EQUATION

The analysis of the pressure generated by lubricant films is almost exclusively performed with a form of the classical Reynolds equation. This differential equation

derives from the inertialess form of the Navier-Stokes equation combined with the continuity equation with the assumption that the flow channel is small in one coordinate direction. It has been generalized to incorporate variable viscosity as well as variable density and has been remarkably accurate in predicting the film thickness in non-conformal contact problems. However, there is a fundamental limitation to the Reynolds equation for problems in which viscosity varies with pressure and in particular, in the elastohydrodynamic regime. The cross-film pressure gradient cannot be neglected and secondary flows result.

Renardy [8] recognized that the Navier-Stokes equations for an incompressible, piezoviscous fluid may suffer from non-existence and nonuniqueness problems when the principal tensorial strain rates are not less than $(2\mu\alpha)^{-1}$. Here, μ is viscosity and $\alpha = d \ln\mu / dp$ is the local pressure viscosity coefficient. The Navier-Stokes equations can undergo a change of type—a process which has been used to characterize shear localization [9].

2. NON-LINEAR SHEAR RESPONSE

The search for the relevant constitutive equations which relate the lubricant stress to the flow kinematics in a concentrated contact has occupied the interest of tribologists working in EHD for at least thirty years. The goal has been to construct experiments to verify the rheological models and to provide the necessary property relations so that the complete elastohydrodynamic solution may be obtained. Various non-Newtonian models (see [3] for a review) have been advanced which provide accurate solutions for the traction over some operating range when the required rheological properties are obtained

from the same traction data. In 1972, Dyson [10] warned that EHD traction research was "enclosed within a tight circle" of fitting parameters to observations without consideration for measurements made outside of EHD. Hopefully, we have broken from the circle.

We may now generate rheological flow curves under conditions of pressure, temperature, and rate of shear which, although still rather restricted, are sufficiently within the realm of EHD to make accurate traction predictions and compare with traction experiments. We have previously interpreted these flow curves as lubricant constitutive behavior. However, in light of the recent observation [4] of mechanical shear bands operating within the lubricant film concurrent with non-linear shear response, this interpretation must be accompanied by a caveat: Rheological flow curves which are generated in plane shear yield an empirical rate equation which is useful in modeling Couette dominated lubrication problems. A rigorous analysis of the EHD problem would require a constitutive equation and a slip criterion such as Mohr-Coulomb [11].

2.1 VISCOUS HEATING IN COUETTE VISCOMETRY

Presently, the most useful rheometer configuration for investigation of high-pressure, high-stress response of the liquid state is that of rotating concentric cylinders. When a liquid is sheared, the viscous work done raises the temperature of the liquid. While the study of this phenomenon is of itself interesting to lubrication, it is to be avoided in a rheological measurement because constitutive behavior excludes processes which result from temperature variation. In previous work [12] concerning Couette devices the authors have emphasized the importance of a low Brinkman No. (through

primarily a small shearing gap) to mitigate the effect of the temperature difference within the liquid film and fast instrument response to control the temperature of the surfaces of the solid boundaries to the film. An alternate experimental approach is to perform a measurement in so short a time that the temperature profile in the film has not had time to develop but at a late enough time that the velocity profile is fully formed. Winter [13] showed that this latter approach requires that the Prandtl No. be large.

An earlier analysis of the combined effect of instrument response time and cylinder heating [12] modeled the cylinders as a lumped heat capacity. It was found that to minimize errors due to this combination the measured stress history should show no thermal softening over a period of time equal to the instrument response time. Later, the evolution of the radial temperature profile within the cylinders was considered [14]. A detailed example of a numerical thermal simulation of one of the high-pressure Couette viscometers used in this laboratory follows.

Only conduction in the radial direction is considered. An appropriate form of the energy equation for the metal cylinders is

$$\frac{\partial^2 T}{\partial r^2} + \frac{1}{r}\frac{\partial T}{\partial r} = \frac{\rho_m C_m}{k_m}\frac{\partial T}{\partial t} \qquad (1)$$

where r is the radial coordinate, t is time and ρ, C, and k are the density, specific heat capacity and thermal conductivity, respectively. The subscript, m, refers to the metal from which the cylinders are fabricated. Within a pressure vessel the outer surface of the outer cylinder (or cup) is in contact with low conductivity liquid. Therefore at the outermost surface the boundary condition is set at $\partial T/\partial r = 0$, namely it is an adiabatic

surface. Symmetry at that axis of rotation dictates a similar boundary condition, $\partial T/\partial r = 0$ at $r = 0$.

The shearing gap is very thin compared with the working radius so that curvature of the liquid film can be ignored. A preliminary numerical solution for the liquid film with isothermal boundaries and dissipation showed that for a 1 μm film, steady state temperature distribution was achieved after 10 μs of shearing. Therefore, the storage term in the energy equation for the liquid film is dropped. Including the dissipation term, $\tau\dot{\gamma}$. we have for the liquid

$$k\frac{\partial^2 T}{\partial r^2} + \tau\dot{\gamma} = 0 \qquad (2)$$

The geometry considered is shown in Figure 1. The liquid being sheared is in the circular gap between the outer and inner cylinders. Only the outer cylinder rotates with a velocity which yields a specified average of the rate of shear, $\dot{\gamma}$. The temperature and the radial heat flux are made continuous at the two metal/liquid interfaces. Equations (1) and (2) in their respective regions are solved numerically with the above boundary conditions and with initial uniform temperature (arbitrarily set to zero for Figure 1) to obtain temperature distribution and shear stress versus time.

The result of a sample computation is shown in Figure 1 for two velocity histories. The velocity of the outer cylinder was increased linearly with time until an apparent or average rate of shear of $10^4 s^{-1}$ was reached at t_o equal to 10 and 50 ms. The liquid rheology was Newtonian with $\mu = 10^3$ Pa·s and $\beta = 0.1°C^{-1}$. The gap was 1.0 μm. The liquid and metal thermal conductivities were $k = 0.15$ and $k_m = 225$ W/m°C and for the metal $\rho_m C_m = 3 \times 10^6$ J/m^3°C. The temperature profiles within the metal cylinders

are shown in Figure 1 for $t = t_o$. The liquid film temperature reached a maximum very near the surface of the inner cylinder. The reduction in shear stress from isothermal was less than 2% for t_o = 10 ms and less than 4% for t_o = 50 ms. The rotational velocity in this example is only about 1 revolution per second and can easily be achieved in 10 ms by a stepper motor. When a very large driving torque is required a 50 ms linear velocity ramp may be necessary.

In early high-pressure Couette devices the critical response time was often that of the torque transducer which provides the stress measurement. This transducer is immersed in a high-pressure liquid and for high viscosity the transducer responds as a first order instrument with a time constant, t_c, which is proportional to liquid viscosity. Very fast measurements may be obtained by accelerating both cylinders and then arresting the rotation of one cylinder with the torque transducer which can be immersed in a low viscosity liquid. Now, the velocity response is intimately connected with the transducer response. The undamped natural frequency for the transducer is 2.5 kHz. Theoretically, a 5 percent settling time [15] of 0.2 ms can be achieved for transducer response by optimizing the damping liquid viscosity. This is difficult to achieve in practice as the viscosity of the damping liquid changes with the test temperature and pressure. In any event, we have not observed an improvement in measurements typical of those reported here when done faster than 50 ms. The temperature increases shown in Figure 1 present no problem in interpretation of results.

Also, by not considering axial conduction in the cylinders the analysis overestimates the metal temperature rise. Comparing measured stress histories for a

Newtonian liquid with the computed stress history at t = ls we found the actual loss of shear stress compared to isothermal shear was only 64% of the predicted loss.

The temperature distribution of Figure 1 was incorporated into a thermal-elastic numerical analysis of each cylinder using both plane-strain and plane-stress idealizations. Thermal expansion results in no subtantial change in the operating film thickness at the time of the measurement.

2.2 SOME RESULTS FOR PRESSURES TO 300 MPA

A high-pressure, high shear stress Couette viscometer was developed [14] in this laboratory to operate at pressures to 300 MPa. The steady shear response of various liquid lubricants [14] and a grease [16] have been investigated. For the grease, an empirical stress equation was found of the form

$$\tau^q = \tau_y^q + (g\mu\dot{\gamma})^q \quad , \tau \geq \tau_y \tag{3}$$

where g is a dimensionless viscosity enhancement factor approximately equal to 2, q is a dimensionless exponent and μ is the base oil viscosity. For q = 0.5, equation (3) becomes Casson's equation for oil/particulate mixtures.

Flow curves are presented for a high-traction fluid, Santotrac 50 and a mineral oil, LVI 260 in Figures 2 and 3, respectively. Although the pressures and temperatures are comparable the shear response is quite different. The cycloaliphatic traction fluid remains Newtonian to a shear stress of at least 10 MPa whereas the mineral oil responds non-linearly above 3 MPa. Note also that for the mineral oil, the stress becomes essentially independent of rate at about τ = 10 MPa and that the temperature dependence diminishes as the rate dependence diminishes. Because of their extended Newtonian

response we have begun to use the cycloaliphatic traction fluids as viscosity standards for shear stress greater than 1 MPa in calibrating cylinder gaps.

2.3 A NEW HIGH-STRESS COUETTE VISCOMETER FOR 600 MPA PRESSURE

An increase in the pressure capability of previous rotating concentric cylinder viscometers is necessary to investigate the shear response of typical lubricants well above the glass transition temperature. Translating concentric cylinder rheometers are capable of pressures above 1 GPa; however the rate of shear is so low that the viscosity must be made very large in order to achieve an interesting magnitude of shear stress. Hence experiments are often conducted near the glass transition of the lubricant.

We recently reported [14] the development of a Couette viscometer for pressure to 300 MPa and the results of the previous section were obtained with that device. The pressure capability of the Couette technique is doubled with the device shown in section view in Figure 4. The outer cylinder (cup) is driven by an external stepper motor by means of a drive shaft. The thrust bearing which prevents expulsion of the shaft from the vessel has been moved to outside of the vessel so that the bearing does not run in pressurized liquid. The high-pressure seal is now a simple spring-loaded packing. There is no need for high-pressure electrical feed-throughs since the torque measurement is transmitted out of the vessel optically. The inner cylinder (bob) is restrained from rotation by a torsion bar with a mirrored surface within a glass tube. See Figure 4.

The principle of the torque measurement is depicted in Figure 5. The twist of the torsion bar results in a deflection of a laser beam which is detected by an optical position sensor. A glass tube (Figure 4) provides a circular interface between the liquid which

surrounds the mirror and the pressurizing fluid so that changes in refractive index of the sample has no effect on the measurement.

2.4 RESULTS FOR PRESSURES TO 600 MPA

A flow chart is presented for the polyalphaolefin, SHF1001, in Figure 6. The response is apparently Newtonian to about 2 MPa shear stress, although the effective viscosity below 2 MPa is slightly reduced compared to falling body measurements.

The mineral oil, HVI 650, has been the subject of numerous traction experiments. The shear response of HVI 650 is depicted in Figures 7 a and b. The curves drawn through the data points for 23°C and 44°C represent the empirical Carreau-Yasuda equation

$$\tau = \mu\dot{\gamma}\left[1 + \left(\frac{\mu\dot{\gamma}}{\tau_L}\right)^a\right]^{(m-1)/a} \tag{4}$$

Here, a is a dimensionless parameter which controls the breadth of the transition from Newtonian to a non-Newtonian flow regime with rate sensitivity coefficient of m. For m = 0, τ_L is a limiting shear stress. In Figures 7 a and b, we used a = 1.5 at 23°C and a = 2 at 44°C. For the limiting stress, the form proposed by Bezot, et al. [17] was adopted

$$\tau_L = c_o + c_1 p + c_2 p^2 \tag{5}$$

Using the results of Figure 7b and Ref [18] and [19], we obtained $c_1 = 0.034$ and $c_2 = 2.1 \times 10^{-5}$ MPa with c_o arbitrarily set to zero. Note that for HVI 650 at 44°C (Figure 7a) the curves are also a good approximation of the Sinh Law,

$$\tau = \tau_o \sinh^{-1}\left(\mu\dot{\gamma} / \tau_o\right) \tag{6}$$

where τ_o is a stress which represents the limit of Newtonian response and is 3.3, 5.2 and 6.5 MPa for pressures of 448, 517 and 586 MPa respectively. That is, $\tau_o \approx \tau_L / 4$ at 44°C.

The shear response of the traction fluid, Santotrac 40, is shown in Figure 8. For the pressure of 414 MPa, the solid curve is equation (4) and the two broken curves are equation (6) for τ_o of 6 and 25 MPa respectively. When elastohydrodynamic traction curves are interpreted in terms of equation (6) together with exponential pressure-viscosity the traction gradient can be set equal to τ_o [18]

$$\frac{\partial \bar{\tau}}{\partial \ell n \dot{\gamma}} = \tau_o \tag{7}$$

Values of τ_o obtained from traction tests using (7) are typically less than 6 MPa [18, 20] for cycloaliphatic traction fluids under conditions of Figure 8. Clearly, from Figure 8. the Newtonian limit exceeds 6 MPa and is close to 25 MPa. Therefore, any interpretation of the traction gradient as a Newtonian limit through a Sinh Law model with τ_o independent of pressure must be suspect. However, if the pressure of a rheological measurement is chosen carefully it should be possible to obtain agreement between the Newtonian limit for that particular pressure and the traction gradient since the Newtonian limit is pressure dependent (eg., HVI 650 at 448 MPa and 44°C).

We have investigated the grease from Ref [16] and its base oil in the current rheometer to explore departures from Newtonian behavior at high shear stress. In Figure 9, for room temperature, the mineral base oil, 600P, is non-Newtonian above τ = 2 MPa at 310 MPa pressure. When the pressure is increased to 517 MPa this oil is Newtonian to τ = 3 MPa. The CA7000, which is a soap-thickened grease of 600P, is also shown in Figure 9. It would appear from these limited data that the shear stress for the grease (at

high stress) may be obtained by multiplying the base oil result by the previously [16] obtained viscosity enhancement factor, g, which is about 2. Clearly, equation (3) is not applicable here since it becomes approximately Newtonian at high shear stress. Other techniques have been developed to probe the response of liquids to high pressure and stress.

Other laboratories have observed rate independence at elevated pressure. For example, the High-Pressure Impact Viscometer of Wong, et. al. [21] entraps a quantity of liquid between a ball and a plate. Interferometry is used to determine the local flow rate of liquid leaking from the entrapment and local surface distortion which yield local pressure from elasticity theory. A Rabinowitsch Correction for slit flow gives the true shear rate at the surface. The authors concluded that the effective viscosity was found in earlier works to be a function of time because the shear rate varied with time while the shear stress remained at the limiting value. Limiting stress type behavior was observed over 4 decades of shear rate with $m \approx 0.01$ for LVI 260.

3. EHD TRACTION CALCULATION

We should expect our property measurements to yield reasonable predictions of concentrated contact traction. Evans [22] generated isothermal, line-contact traction curves for three of the most widely investigated liquid lubricants: 5P4E, Santotrac 50 and HVI650. These data were described as isothermal since the disc temperature was adjusted to provide a constant estimated average film temperature. These traction data are presented for HVI650 in Figure 10 for inlet temperatures of 40 and 60°C and average

pressures, $\bar{p}$, of 0.47 and 0.63 GPa. The sliding velocity is ΔU and inlet temperature rise is 3°C.

For the traction calculations which are the curves in Figure 10, we assumed the Hertzian pressure distribution and integrated the Carreau-Yasuda equation (4) across the contact area to obtain the average shear stress, $\bar{\tau}$. The dimensionless parameter, a, was specified by a = 63/(T+19°C) which yields the values obtained in the previous section without approaching the meaningless condition of a = 0 at ordinary temperatures. Viscosity was obtained from a Free Volume Model [23] and limiting stress was obtained from equation (5). Results were insensitive to the selection of the rate sensitivity, m, from 0 to 0.03. Although the predicted curve at 40°C rolls over more quickly than the measured traction, the general agreement is good. Considering the great differences between the two techniques and the assumptions involved (eg., dry Hertzian pressure distribution) it might be unreasonable to expect to do better.

4. MECHANICAL SHEAR BANDS IN NON-VISCOMETRIC FLOW

It has long been suspected that the rate independent behavior observed and discussed above was related to slip; either at the boundaries, or internal in the material. Visualization of shear bands has to date been accomplished between parallel plates [4]. The interpretation of the flow field and stress state leading up to localization is the least ambiguous for plane Couette shear. This is not however the general case for lubrication flows. To investigate the generation of shear bands in wedge flow we fabricated a new stationary shaft for the High-Pressure Flow Visualization Cell [4]. The stationary surface (the lower surface of Figure 11) was ground at an angle of 5° with the direction of motion of the moving (upper of Figure 11) surface. Observation of birefringence during shear through crossed polarizers clearly showed a shear stress gradient across the film as expected. Shear bands appeared as shown in Figure 11 for 5P4E. These bands are similar to those observed between parallel plates. However, the Mohr-Coulomb analysis can not easily be applied because of the non-uniform stress field in the film. In solid mechanics isothermal shear bands are often associated with a change in type of the governing partial differential equations. Singularities in the governing equations accompany this change of type. As shown below, singularities do occur in the Navier-Stokes equation with realistic lubricant properties.

5. A FUNDAMENTAL LIMITATION OF THE REYNOLDS EQUATION FOR PIEZOVISCOUS LIQUIDS

We have just seen that shear bands will develop during non-Viscometric shear of a lubricant at high pressure and high-shear stress. These visible bands effectively represent slip planes and are not predicted by current numerical analyses of lubricant behavior.

The analysis of the pressure generated by lubricant films is almost exclusively performed with a form of the classical Reynolds equation. This differential equation derives from the

inertialess form of the Navier-Stokes equation combined with the continuity equation with the assumption that the flow channel is small in one coordinate direction. It has been generalized to incorporate variable viscosity as well as variable density and has been remarkably accurate in predicting the film thickness in non-conformal contact problems. However, there is a fundamental limitation to the Reynolds equation for problems in which viscosity varies with pressure and in particular the regime of elastohydrodynamics. The cross-film pressure gradient cannot be neglected, and secondary flows result even for flow between parallel plates.

Renardy recognized [8] that the Navier-Stokes equations for an incompressible, piezoviscous fluid may suffer from non-existence and nonuniqueness problems when the principal tensorial strain rates are not less than $(2\mu\alpha)^{-1}$. Here, μ is viscosity and α=d ln μ/dp is the local pressure viscosity coefficient where p is the pressure. The Navier-Stokes equations can undergo a change of type - a process which has been used to characterize shear localization [9].

Recently, Bair and Khonsari [24] reported the occurrence of singular pressure gradients in two-dimensional, inhomogeneous flows of incompressible piezoviscous liquids. In the case of flow between parallel plates, these singularities were shown to take place when the shear stress τ approaches $1/\alpha$. This criterion is equivalent to that found by Renardy. Note that the one-dimensional Reynolds equation does not yield this singularity. In fact it predicts a trivial solution for the pressure if pressure boundary conditions are fixed at a constant value. We will show that the pressure dependence of viscosity leads to very large cross film pressure gradients and secondary flows.

5.1 PIEZOVISCOUS REYNOLDS EQUATION

Consider the derivation of a generalized Reynolds equation by Dowson [25]. The coordinate system is defined so that z is in the direction of the film thickness h. The x and y dimensions of the bearing are of the order of L which is several orders of magnitude greater than h. Following Dowson, the first stage of the order of magnitude analysis of the Navier-Stokes equations for a Newtonian liquid yields:

$$\frac{\partial p}{\partial x} = \frac{\partial}{\partial z}\left(\mu \frac{\partial u}{\partial z}\right) \tag{8}$$

and a similar equation for $\partial p/\partial y$.

For the cross-film direction, the appropriate equation is:

$$\frac{\partial p}{\partial z} = \cdots + \frac{\partial}{\partial x}(\mu \frac{\partial u}{\partial z}) \qquad (9)$$

where we will assume that the terms represented by ... are of lesser magnitude than the term retained. In arriving at these equations it is apparently assumed that in general a function such as $\partial\varphi/\partial\xi$ is of the order of φ/ξ. Then if z is of the order of h_o, comparing only the right hand sides of (8) and (9) gives the result that $(\partial p/\partial z)/(\partial p/\partial x)$ is of the order of h_o/L. This result is usually used to justify the omission of $\partial p/\partial z$., but clearly the left-hand side gives the opposite result.

To illustrate the significance of the cross flow pressure gradient, we carry out the differentiation of the products in the right-hand sides of (8) and (9) as shown below:

$$\frac{\partial p}{\partial x} = \alpha\mu \frac{\partial p}{\partial z}\frac{\partial u}{\partial z} + \mu \frac{\partial^2 u}{\partial z^2} \qquad (8a)$$

$$\frac{\partial p}{\partial z} = \cdots + \alpha\mu \frac{\partial p}{\partial x}\frac{\partial u}{\partial z} + \mu \frac{\partial^2 u}{\partial x \partial z} \qquad (9a)$$

Begin with an inspection of (9a). We neglect the term involving cross derivatives since $\partial u/\partial x$ is expected to be small; however, our argument is not compromised if this term is included. Applying a similar order-of-magnitude rule as before shows that the ratio $(\partial p/\partial z)/(\partial p/\partial x)$ is of the order of $\alpha\mu U/h_o$. A conservative value of α is $10^{-8}Pa^{-1}$. Taking the velocity in the x-direction, U, to be 1 m/s and h_o to be 10^{-7} m, we find that with a viscosity evaluated at low pressures, say $\mu=10^{-2}$ Pa.s, the order of magnitude of $(\partial p/\partial z)/(\partial p/\partial x)$ is 10^{-3}. This is typical of hydrodynamic lubrication or EHL inlet zones and this order of magnitude analysis can be used to neglect the pressure gradient in the cross film direction. For pressures relevant to Hertzian zone, $\mu=10^{4}$ Pa.s is not unusual and the order of magnitude of $(\partial p/\partial z)/(\partial p/\partial x)$ becomes 10^{3}. Clearly, therefore, at high pressures $\partial p/\partial z$ is not insignificant compared to $\partial p/\partial x$.

In deriving the classical Reynolds equation based on the reduced form of the Navier-Stokes equation, it is typical to define a dimensionless viscosity as $\bar{\mu} = \mu/\mu_o$, where $\bar{\mu}$ is assumed to be of the order of one. If μ_o is taken to be ambient viscosity, then $\bar{\mu}$ can be very large at high pressures. Even when the cross film gradient is significant, it must have an affect on the pressure profile calculation for us to question the use of Reynolds equation for

elastohydrodynamic applications. Notice that in equation (8a) the term $\partial p / \partial z$ appears explicitly and that it is coupled to $\partial p / \partial x$. This coupling can result in a singularity in the pressure gradient which the Reynolds equation is incapable of predicting.

5.2. LUBRICANT PROPERTIES

Before developing some properties of the isothermal piezoviscous Navier-Stokes equations for the Hertzian zone, it is instructive to examine the viscosity and compressibility of liquid lubricants at very high pressure. Free volume models are useful for lubrication analyses because they provide a link between volume and viscosity. In the following example, we make use of the isothermal free volume model of Cook, et al. [27].

The Dolittle equation relates viscosity to volume, V, and occupied volume, V_{occ}.

$$\ln \mu = \frac{BV_{occ}}{V - V_{occ}} - \frac{BV_{occ}}{V_o - V_{occ}} + \ln \mu_o \tag{10}$$

The Tait equation provides an expression of the volume variation with pressure:

$$\frac{V}{V_o} = 1 - \frac{1}{K_o' + 1} \ln\left(1 + p\frac{(1 + K_o')}{K_o}\right) \tag{11}$$

At zero pressure the volume is V_o, the bulk modulus is K_o and the pressure rate of change of the bulk modulus is K_o'. The secant compressibility is then

$$\Phi_s = -\frac{1}{V_o}\frac{dV}{dp} = \frac{1}{K_o + (1 + K_o')p} \tag{12}$$

It can be shown empirically that V_{occ} is nearly independent of pressure. Differentiating (10) yields:

$$\alpha = \frac{\beta \dfrac{V_{occ}}{V_o}}{\left(\dfrac{V}{V_o} - \dfrac{V_{occ}}{V_o}\right)^2} \Phi_s \tag{13}$$

Parameters typical of a mineral oil at a temperature of 75°C, are B=3, K_o=1.5 GPa K'_o=10 and V_{occ}/V_o=0.70.

A plot of Φ_s and α as a function of pressure is shown in Figure 12. First note the remarkable reduction of compressibility for increasing pressures. Although the existence of high

pressure is often a justification for a compressible solution, if we restrict our attention to pressures greater than 1 GPa, an incompressible analysis is acceptable. Note also that following a slight decrease at low pressures, α increases with pressure for pressures greater than about 0.5 GPa. This is a result of the competition between the rapidly decreasing compressibility at low pressures which decreases the sensitivity of viscosity to pressure and the reduction of free volume at high pressures which increases the sensitivity of viscosity to pressure. (Liquids for which K_o is particularly high will not show the initial decrease of α with p.) The pressure-viscosity coefficient can be very large at high pressures. This is in contradiction with empirical rules often used in EHD numerical simulations for which α is allowed to monotomically decrease with pressure.

The analyses which follow pertain to applications where the pressure is high enough so that compressibility of the liquid can be neglected and that the shear stress is comparable to the reciprocal of α. To make the piezoviscous Navier-Stokes equations tractable, we will treat α as a constant. recognizing that this assumption is an idealization.

5.3 Navier-Stokes Equations for Two-Dimensional, Intertialess Flow of an Incompressible, Piezoviscous Liquid

Consider the creeping flow of a liquid for which the flow channel is very large in one direction, y. The component of the velocity in the y-direction, v, and all derivatives with respect to y must be zero to provide symmetry. The appropriate Navier-Stokes equations are:

$$\frac{\partial p}{\partial x} = \frac{\partial}{\partial x}\left[2\mu\frac{\partial u}{\partial x} + \left(\varsigma - \frac{2}{3}\mu\right)\left(\frac{\partial u}{\partial x} + \frac{\partial w}{\partial z}\right)\right] + \frac{\partial}{\partial z}\left[\mu\left(\frac{\partial w}{\partial x} + \frac{\partial u}{\partial z}\right)\right] \tag{14}$$

$$\frac{\partial p}{\partial z} = \frac{\partial}{\partial z}\left[2\mu\frac{\partial u}{\partial z} + \left(\varsigma - \frac{2}{3}\mu\right)\left(\frac{\partial u}{\partial x} + \frac{\partial w}{\partial z}\right)\right] + \frac{\partial}{\partial x}\left[\mu\left(\frac{\partial w}{\partial x} + \frac{\partial u}{\partial z}\right)\right] \tag{15}$$

where ς is the bulk viscosity which is not zero for liquids.

The continuity equation for an incompressible liquid reads:

$$\frac{\partial u}{\partial x} + \frac{\partial w}{\partial z} = 0. \tag{16}$$

Using equation (9), the Navier-Stokes equations (7) and (8) reduce to the following form:

$$\frac{\partial p}{\partial x} = 2\frac{\partial}{\partial x}\left(\mu u_x\right) + \frac{\partial}{\partial z}\left[\mu\left(w_x + u_z\right)\right] \tag{17}$$

$$\frac{\partial p}{\partial z} = 2\frac{\partial}{\partial z}\left(\mu w_z\right) + \frac{\partial}{\partial x}\left[\mu\left(w_x + u_z\right)\right] \tag{18}$$

where subscripts on velocities represent partial differentiation.

Note that

$$\frac{\partial \mu}{\partial x} = \alpha\mu\frac{\partial p}{\partial x} \text{ and } \frac{\partial \mu}{\partial z} = \alpha\mu\frac{\partial p}{\partial z} \tag{19}$$

Substitution and differentiation gives

$$\frac{\partial p}{\partial x} = 2\mu\alpha\, u_x\frac{\partial p}{\partial x} + \mu\alpha\left(u_z + w_x\right)\frac{\partial p}{\partial z} + \mu\nabla^2 u \tag{20}$$

$$\frac{\partial p}{\partial z} = 2\mu\alpha\, w_z\frac{\partial p}{\partial z} + \mu\alpha\left(u_z + w_x\right)\frac{\partial p}{\partial x} + \mu\nabla^2 w \tag{21}$$

Components of the strain-rate tensor are:

$$d_{i,j} = \frac{1}{2}\left(\frac{\partial u_i}{\partial x_j} + \frac{\partial u_j}{\partial x_i}\right), \tag{22}$$

with principal values of 0, d_1, and $-d_1$, where for this problem

$$d_1^2 = d_{zx}^2 - d_{xx}d_{zz} \tag{23}$$

Equations (20) and (21) can be combined to give the following result which uses the above notation.

$$\frac{\partial p}{\partial x} = \frac{\mu\left[2\mu\alpha d_{xz}\nabla^2 w + (1-2\mu\alpha d_{zz})\nabla^2 u\right]}{1-(2\mu\alpha d_1)^2} \tag{24}$$

$$\frac{\partial p}{\partial z} = \frac{\mu\left[2\mu\alpha d_{xz}\nabla^2 u + (1-2\mu\alpha d_{xx})\nabla^2 w\right]}{1-(2\mu\alpha d_1)^2} \tag{25}$$

Clearly for $\alpha = 0$, $\frac{dp}{dx} = \mu\nabla^2 u$ and $\frac{dp}{dz} = \mu\nabla^2 w$ as required. Note that there may be singular pressure gradients for

$$d_1 = \frac{1}{2\mu\alpha} \tag{26}$$

An equivalent expression for (26) is:

$$\tau_1 = \frac{1}{\alpha}, \tag{27}$$

where τ_1 is the maximum principal shear stress.

5.4 Example

Consider the two-dimensional flow of an incompressible piezoviscous liquid between two parallel plates with in-plane realtive motion. The cross-film direction is the z-direction with thickness h_o and plate motion is in the x-direction. For the isoviscous case the velocity profile is parabolic and the x component of velocity is a function of z only. For no wall slip and z=0 at one plate and for an isoviscous liquid, the components of the velocity should be of the forms given below:

$$u(z) = az + bz^2$$

$$w = 0. \tag{28}$$

It has been customary to assume the velocity field given by (28) for piezoviscous fluids. We will show later that in the case of flow between parallel plates a secondary flow must exist when the viscosity is a function of pressure. For illustrative purposes, however, we will assume that $w \equiv 0$ is a good approximation.

Equation (24) and (25) can be written in terms of velocities as:

$$\frac{\partial p}{\partial x} = \frac{\mu}{D}\left[\left(1 - 2\alpha\mu w_z\right)\nabla^2 u + \alpha\mu\left(w_x + u_z\right)\nabla^2 w\right] \tag{24}$$

$$\frac{\partial p}{\partial z} = \frac{\mu}{D}\left[\left(1 - 2\alpha\mu u_x\right)\nabla^2 w + \alpha\mu\left(w_x + u_z\right)\nabla^2 u\right] \tag{25}$$

with

$$D = 1 + (\mu\alpha)^2\left[4u_x w_z - (w_x + u_z)^2\right] \tag{29}$$

Substituting w = 0, we obtain

$$\frac{\partial p}{\partial x} = \frac{\mu u_{zz}}{1 - (\alpha\mu u_z)^2} \tag{30}$$

$$\frac{\partial p}{\partial z} = \frac{\alpha\mu^2 u_z u_{zz}}{1 - (\alpha\mu u_z)^2} = \alpha\mu u_z \frac{\partial p}{\partial x} \tag{31}$$

Introduce the dimensionless quantities

$$\bar{p} = (p - p_R)\alpha : \bar{x} = (x - x_r)\mu_R u_{zz}\alpha ; \bar{\mu} = \frac{\mu}{\mu_R} = e^{\bar{p}} ; T = u_z \alpha \mu_R , \tag{32}$$

where subscript R denotes a reference value at $\bar{x} = 0$.

We will solve equation (30) along a constant z plane. Using the dimensionless quantities defined in (32). equation (30) reads:

$$\frac{\partial \bar{p}}{\partial \bar{x}} = \frac{e^{\bar{p}}}{1 - T^2 e^{2\bar{p}}} \tag{30a}$$

which is separable. Integrating (30a) and making use of the boundary condition $\bar{p}(\bar{x} = 0) = 0$, leads to

$$\bar{x} = 1 + T^2 - e^{-p} - T^2 e^{\bar{p}} \tag{33}$$

which can be solved for $\bar{p}$ as

$$e^{\bar{p}} = \frac{-S \pm \sqrt{S^2 - 4T^2}}{2T} \tag{34}$$

where $S = \bar{x} - 1 + T^2$.

Figure 13 depicts the variation of $\bar{p}$ as a function of $\bar{x}$ for T = 0 and T = 0.5. Notice that for $\bar{x} > (1 - T)^2$, there is no real solution for the pressure. Notice also that there are two branches

of $\bar{p}(\bar{x})$, although the upper branch may be discarded as it does not satisfy the boundary condition.

Turning our attention now to the Reynolds equation for the piezoviscous flow of a liquid between parallel plates we can write

$$\frac{d}{dx}\left(\frac{1}{\mu}\frac{dp}{dx}\right) = 0 \tag{35}$$

Integration of (35) results in the following.

$$\frac{dp}{dx} = C\mu = \mu u_{zz} \tag{36}$$

where the constant of integration, C, is u_{zz}. Therefore in dimensionless form, equation (36) reads:

$$\frac{d\bar{p}}{d\bar{x}} = e^{\bar{p}} \tag{36a}$$

The above solution is the same as that predicted by equation (30a) with T=0, which is shown in Figure 13. Comparison of the right-hand-side of (30) with that of (36) reveals that the Reynolds equation adequately captures the mechanics of a piezoviscous liquid only when $\alpha \mu u_z << 1$ (in other words $\alpha \tau << 1$) assuming w=0.

5.5. SECONDARY FLOWS

In the previous example, it was tacitly assumed that for flow between parallel plates, the component of the velocity normal to the boundary, w, is zero. This is true for isoviscous flows and can be easily verified. For Piezoviscous flows, this assumption allows great simplification of the Navier-Stokes equations and is analogous to the result obtained by Denn [26] for cylindrical Poiseuille flow. However, we will show that neglecting the cross-film velocity component in a flow of a piezoviscous fluid between parallel plates results in inconsistent cross-derivatives of pressure. To illustrate, we will begin by examining the cylindrical Poiseuille flow.

5.5.1 CYLINDRICAL POISEUILLE FLOW

Denn [25] used a perturbation solution to establish that the radial velocity, v, was zero in cylindrical flow. In preparation for the following section, we will obtain Denn's result by different means.

For isoviscous liquids, the velocity is of the form

$$u = q\frac{R^2}{2} - q\frac{r^2}{2} \tag{37}$$

and $$v = 0$$

where R is the radius of the cylindrical duct and $q = 4Q/\pi R^4$, where Q is the flow rate.

The appropriate Navier-Stokes equations for an incompressible piezoviscous liquid are:

$$\frac{\partial p}{\partial \xi} = \alpha\mu\frac{\partial u}{\partial r}\frac{\partial p}{\partial r} + \frac{\mu}{r}\frac{\partial u}{\partial r} + \mu\frac{\partial^2 u}{\partial r^2} \tag{38}$$

$$\frac{\partial p}{\partial r} = \alpha\mu\frac{\partial p}{\partial x}\frac{\partial u}{\partial r} \tag{39}$$

where r and ξ represent the radial and axial directions, respectively.

Making use of (37). equations (38) and (39) become

$$\frac{\partial p}{\partial \xi} = -\alpha\mu q r\frac{\partial p}{\partial r} - 2\mu q \tag{40}$$

$$\frac{\partial p}{\partial r} = -\alpha\mu q r\frac{\partial p}{\partial \xi} \tag{41}$$

Combining,

$$\frac{\partial p}{\partial \xi} = \frac{-2\mu q}{1-(\alpha\mu q r)^2} \tag{42}$$

$$\frac{\partial p}{\partial r} = \frac{2\alpha r\mu^2 q^2}{1-(\alpha\mu q r)^2} \tag{43}$$

Taking the partial derivatives of (42) and (43), we obtain the following equations.

$$\frac{\partial}{\partial r}\left(\frac{\partial p}{\partial \xi}\right) = 2\alpha\frac{\partial p}{\partial \xi}\frac{\partial p}{\partial r} + r\alpha^2\left(\frac{\partial p}{\partial r}\right)^2\left(\frac{\partial p}{\partial \xi}\right) \tag{37}$$

Take the partial derivative of (36) with respect to ξ to obtain:

$$\frac{\partial}{\partial \xi}\left(\frac{\partial p}{\partial r}\right) = 2\alpha \frac{\partial p}{\partial \xi}\frac{\partial p}{\partial r} + r\alpha^2\left(\frac{\partial p}{\partial r}\right)^2\left(\frac{\partial p}{\partial \xi}\right) \tag{45}$$

The equivalence of the expressions (44) and (45) for the cross derivative of pressure ensures that the solution for p is independent of the integration path taken and verifies the assumed velocity field given by equation (37). Therefore there is no secondary flow, $v \equiv 0$. Note also that in capillary flow, a pressure singularity occurs where $\alpha \mu q r = 1$ and that this singularity will be downstream of the location of the unbounded pressure associated with piezoviscous choking of flow.

5.5.2 Flow Between Parallel Plates

We will take the same approach to investigate secondary flow between parallel plates. Here the kinematics can be made more general as the plates may move relative to one another in the x-direction. We will assume a more general form for the velocity field than the customary parabolic form of equation (28). Here we assume

$$u = u(z) \text{ and } w \equiv 0 \tag{46}$$

Remember $v \equiv 0$, since this is a two-dimensional problem. Recall that the pressure gradients are given by (24) and (25) in general and by (30) and (31) when $w \equiv 0$.

$$\frac{\partial p}{\partial x} = \frac{\mu u_{zz}}{1-(\alpha \mu u_z)^2} \tag{30}$$

$$\frac{\partial p}{\partial z} = \frac{\alpha \mu^2 u_z u_{zz}}{1-(\alpha \mu u_z)^2} = \alpha \mu u_z \frac{\partial p}{\partial x} \tag{31}$$

Differentiating (30) with respect to z yields after much manipulation,

$$\frac{\partial}{\partial z}\left(\frac{\partial p}{\partial x}\right) = 3\alpha \frac{\partial p}{\partial z}\frac{\partial p}{\partial x} + \frac{u_{zzz}}{u_{zz}}\frac{\partial p}{\partial x} + 2\alpha^2 \frac{u_z}{u_{zz}}\left(\frac{\partial p}{\partial z}\right)^2 \frac{\partial p}{\partial x} \tag{47}$$

Similarly, differentiating (24) with respect to x yields

$$\frac{\partial}{\partial x}\left(\frac{\partial p}{\partial z}\right) = 2\alpha \frac{\partial p}{\partial z}\frac{\partial p}{\partial x} + \left(\frac{u_{zx}}{u_z} + \frac{u_{zzx}}{u_{zz}}\right)\frac{\partial p}{\partial z} + \frac{2\alpha}{u_{zz}}\left(\frac{\partial p}{\partial z}\right)^2\left(\alpha u_z \frac{\partial p}{\partial x} + u_{zx}\right) \qquad (48)$$

And with $u_x = 0$, Equation (48) becomes

$$\frac{\partial}{\partial x}\left(\frac{\partial p}{\partial z}\right) = 2\alpha \frac{\partial p}{\partial z}\frac{\partial p}{\partial x} + \frac{2\alpha^2 u_z}{u_{zz}}\left(\frac{\partial p}{\partial z}\right)^2 \frac{\partial p}{\partial x} \qquad (49)$$

Equating the RHS of (49) and (47) reveals properties of the admissible form of $u(z)$ when $w \equiv 0$.

$$u_{zzz} = -\alpha u_{zz}\frac{\partial p}{\partial z} = -\alpha^2 \mu u_z u_{zz}\frac{\partial p}{\partial x} \qquad (50)$$

It is clear that the customary parabolic form of the velocity is inappropriate for $\alpha \neq 0$, since for a polynomial representation of $u(z)$, a third degree term is needed for $\partial^3 u/\partial z^3$ to be nonzero.

Additional information can be extracted by considering that $\partial u_{zzz}/\partial x = 0$, since $w \equiv 0$. Now,

$$-\alpha^2 u_z u_{zz}\left[\alpha\mu\left(\frac{\partial p}{\partial x}\right)^2 + \mu\frac{\partial^2 p}{\partial x^2}\right] = 0 \qquad (51)$$

So that

$$\alpha\left(\frac{\partial p}{\partial x}\right)^2 = \frac{-\partial^2 p}{\partial x^2} \tag{52}$$

Differentiating eqn. (30) with respect to x gives

$$\frac{\partial}{\partial x}\left(\frac{\partial p}{\partial x}\right) = \alpha\left(\frac{\partial p}{\partial x}\right)^2 + 2\alpha^3\mu\frac{u_z^2}{u_{zz}}\left(\frac{\partial p}{\partial x}\right)^3 \tag{53}$$

Substituting (53) into (52) yields

$$u_{zz} = -\alpha^2\mu u_z^2\frac{\partial p}{\partial x} \tag{54}$$

which must be satisfied for $w \equiv 0$. Note that the sign of u_{zz} must be opposite that of $\partial p/\partial x$. This is contrary to what is found in practice. Substituting the expression for $\partial p/\partial x$ (eqn. (30)) into (54) to obtain

$$1 - \alpha^2\mu^2 u_z^2 = -\alpha^2\mu^2 u_z^2 \tag{55}$$

which is, of course, a contradiction. Therefore, $w \not\equiv 0$, and a secondary flow must occur for $\alpha \neq 0$ when a Poiseuille component exists.

6. SUMMARY AND CONCLUSIONS

If care is taken to avoid or correct for viscous heating, the results from high-pressure Couette rheometers may be used to generate empirical rate equations which are useful in modeling elastohydrodynamic traction. This approach, however, fails to ellucidate the details of lubricant flow in the concentrated contact. The outstanding problems of surface roughness effects and EHD related boundary lubrication await analytical techniques which can handle the change in character of the governing (Navier-Stokes) equations.

An analytical treatment of piezoviscous liquids is presented which reveals that the Reynolds equation adequately captures the mechanics of a piezoviscous fluid only when $\tau\alpha \ll 1$. In the elastohydrodynamic lubrication regime, this condition is satisfied in the inlet zone where typically $\tau\alpha \cong 0.02$. Consequently, Reynolds-based EHD inlet analyses yield realistic predictions for film thickness. In the Hertzian contact region, the contribution of the pressure gradient across the film may play a very important role and the use of the Reynolds equation is

questionable. While the mathematical treatment of the subject becomes considerably more complex, these issues must be dealt with if closure is expected in predicting EHD traction and relating it to independently determined lubricant properties.

REFERENCES

1. J.F. Dill, P.W. Drake and T.A. Litovitz, "The Study of Viscoelastic Properties of Lubricants Using High-Pressure Optical Techniques," ASLE Trans., 18, 3, (1975) 202-210.

2. A.J. Barlow, G. Harrison, J.B. Irving, M.G. Kim, J. Lamb and W.C. Pursley, "The Effect of Pressure on the Viscoelastic Properties of Liquids," Proc. Roy. Soc. London A. 327, (1972) 403-412.

3. S. Bair and W.O. Winer, "The High-Pressure, High-Shear Stress Rheology of Liquid Lubricants," Trans. ASME, J. of Tribology, 114, 1, (1992) 1-13.

4. S. Bair, F. Qureshi and W.O. Winer, "Observations of Shear Localization in Liquid Lubricants Under Pressure," Trans. ASME, J. of Tribology, 115, 3, (1993) 507-514.

5. A. Eastwood and G. Harrison, "Non-Newtonian Viscosity at High Stresses," Proc. VIII Intern. Congress Rheology, (1980) 199.

6. S. Clyens, C.R. Evans and K.L. Johnson, "Measurement of the Viscosity of Supercooled Liquids at High Shear Rates with a Hopkinson Bar," Proc. R. Soc. Lond. A381. (1982) 195-214.

7. J. Jakobsen and W.O. Winer, "High Shear Stress Behavior of Some Representative Lubricants," Trans. ASME, JOLT 97, 3, (1975) 479-484.

8. Renardy, M. (1986) "Some Remarks on the Navier-Stokes Equations with a Pressure-Dependent Viscosity," Communications in partial Differential Equations, V. 11, No. 7, pp. 779-793.

9. Lee, Y.K., Ghosh, J., Bair, S., and Winer, W.O. (1994) "Shear Band Analysis for Lubricants Based on a Viscoelastic Plasticity Model" Applied Mechanics Review, V.47, No. 6, AS209.

10. A. Dyson, Interdisciplinary Approach to Liquid Lubricant Technology, Ed. by P. M. Ku, NASA, (1972) 303.

11. S. Bair and W. O. Winer, "A Rheological Basis for Concentrated Contact Friction," Proc. Leeds-Lyon Symp. (1993).

12. S. Bair and W.O. Winer, "The High Shear Stress Rheology of Liquid Lubricants at Pressures of 2 to 200 MPa," ASME J. of Tribology, 112, 2, (1990) 246-252.

13. H.H. Winter, "The Unsteady Temperature Field in Plane Couette Flow," Int. J. Heat Mass Transfer, 14, (1971) 1203-1212.

14. S. Bair and W.O. Winer, "A New High-Pressure, High-Shear Stress Viscometer and Results for Lubricants," Trib. Trans. 36, 3 (1993).

15. E.O. Doebelin, Measurement Systems: Application and Design, McGraw-Hill, New York (1966).

16. S. Bair, "The High-Pressure Rheology of a Soap-Thickened Grease," STLE Trib. Trans. 93-TC-4D-1 (1993).

17. P. Bezot, C. Hesse-Bezot, G. Dalmaz, P. Taravel, P. Vergne and D. Berthe, "A Study of Traction in EHL: Experimental and Simulated Curves for a Silicone Fluid," Wear123, (1988) 13-31.

18. C.R. Evans and K.L. Johnson, "The Rheological Properties of EHD Lubricants," Proc. Instn. Mech. Engrs. 200, No. C5 (1986).

19. S. Bair and W.O. Winer, "Some Observations in High-Pressure Rheology of Lubricants," ASME Journal of Lubrication Technology, 104, 3, (1982) 382-386.

20. M. Muraki, "Molecular Structure of Synthetic Hydrocarbon Oils and Their Rheological Properties Governing Traction Characteristics," Trib. International 20, 6, (1987) 352.

21. P.L. Wong. S. Lingard and A. Cameron, "The High Pressure Impact Microviscometer," STLE Trib. Trans. 35, 3, (1992) 500-508.

22. C.R. Evans, "Measurement and Mapping of the Rheological Properties of EHD Lubricants," Ph.D. Thesis, Cambridge (1983).

23. Bair, S. and Winer, W.O. "Application of the Yasutomi Free Volume Model to Various Liquid Lubricants," Proc. International Symp. Tribology, Yokohama (1995).

24. Bair, S. and Khonsari, M. (1996) "On an Apparent Singularity in the Flow of Liquids Under High Shear Stress," ASME Symposium on Rheology and Fluid Mechanics of Non-linear Materials, paper number G01021, Atlanta, Georgia.

25. Dowson, D. (1962) "A Generalized Reynolds Equation for Fluid-Film Lubrication," International Journal of Mechanical Engineering Sciences, V. 4, pp. 159-170.

26. Denn, M. (1981) "Pressure Drop-Flow Rate Equation for Adiabatic Capillary Flow with a Pressure and Temperature-Dependent Viscosity," Polymer Engineering Science, V. 21, No. 2, pp. 65-68.

27. Cook, R.L., Herbdst, C.A. and King, H.E. (1993) "High-Pressure Viscosity of Glass-Forming Liquids Measured by the Centrifugal Force, Diamond Anvil Cell Viscometer," Journal of Physical Chemistry, V. 97, No. 10, p. 2359.

List of Figures

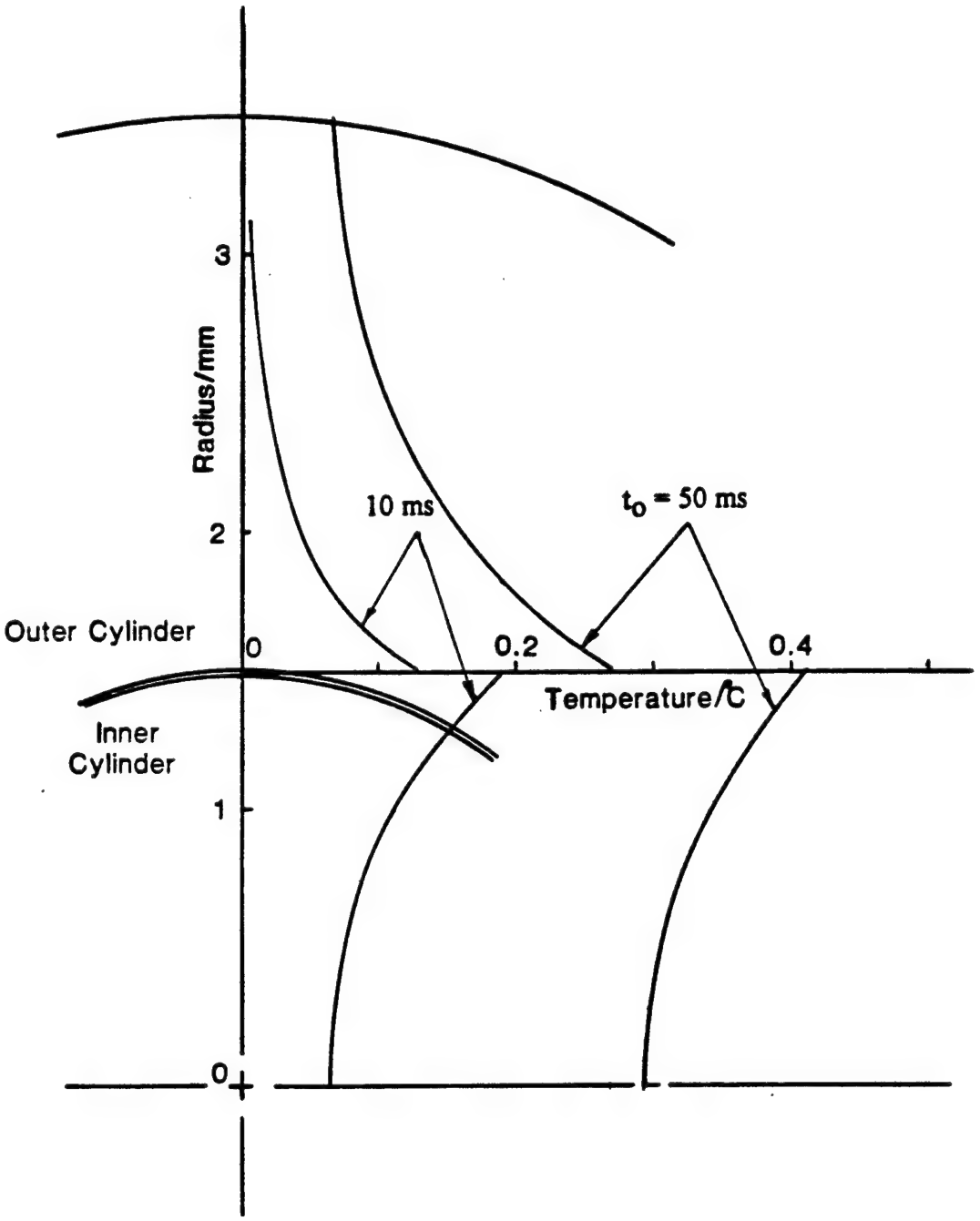

Figure 1 **Radial Temperature Distribution in Concentric Cylinders after Velocity Ramp Lasting for Time, t_o. Result for $t = t_o$**

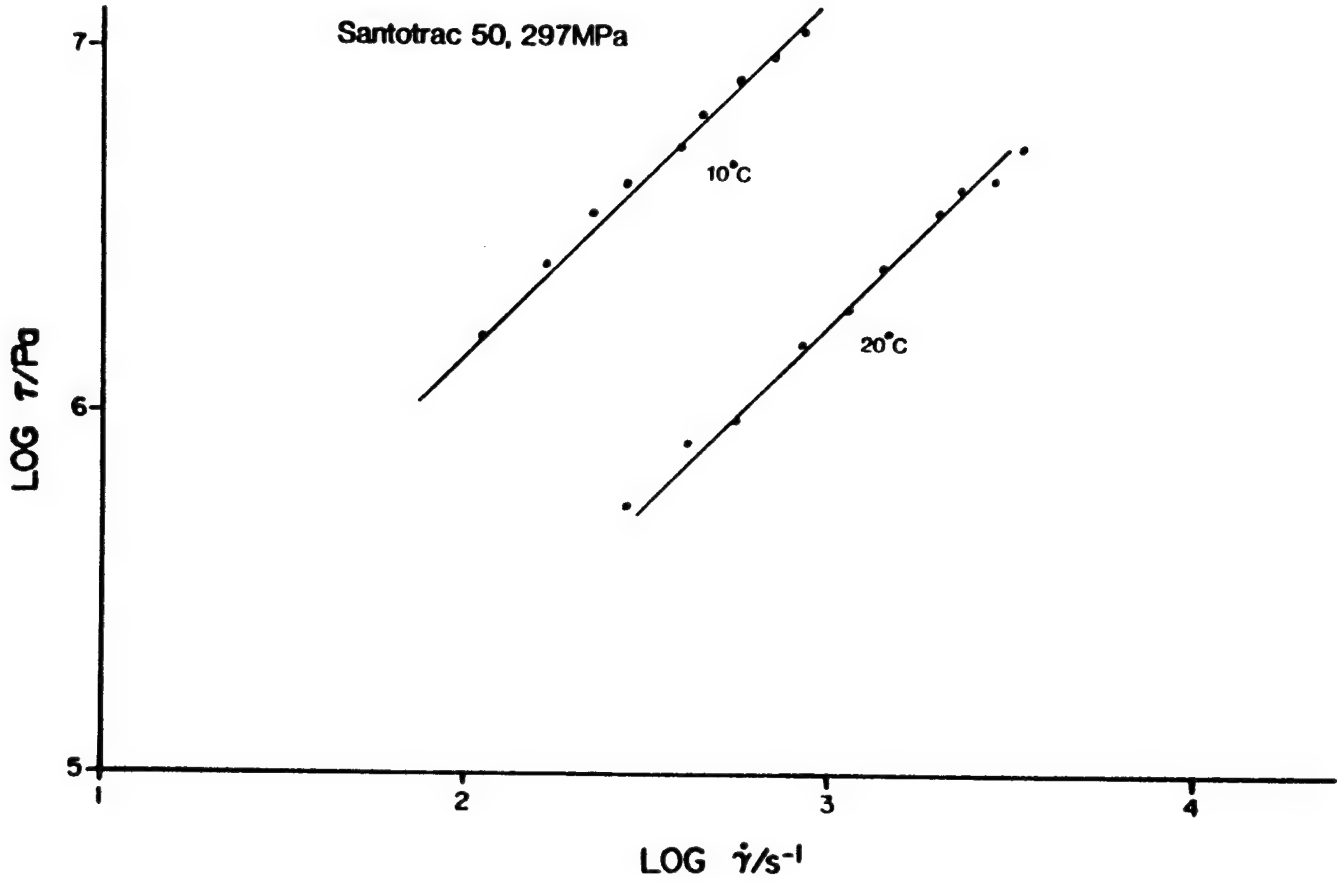

Figure 2. Flow Chart for Santotrac 50, p = 297 MPa.

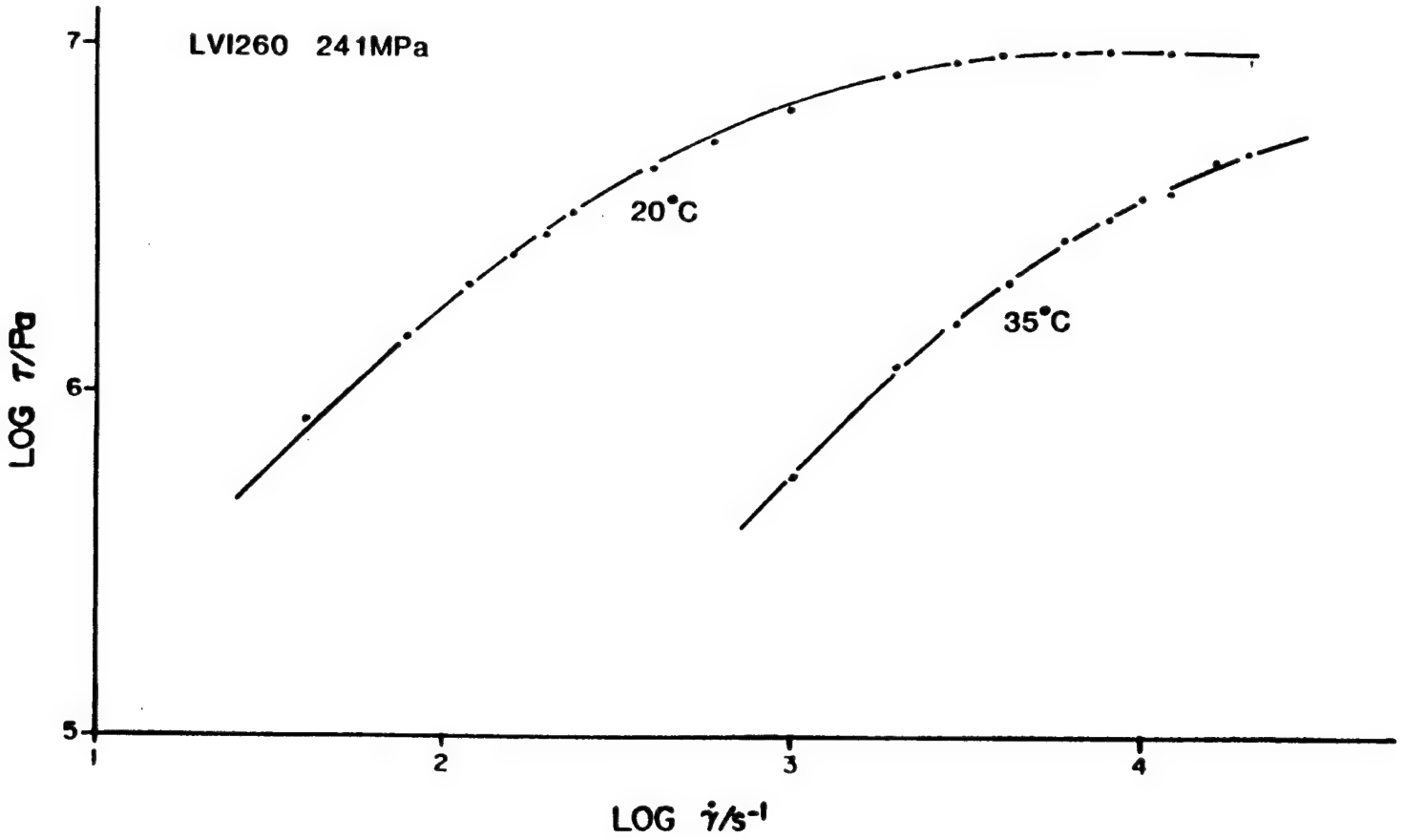

Figure 3. Flow Chart for Mineral Oil, LVI 260, p = 241 MPa.

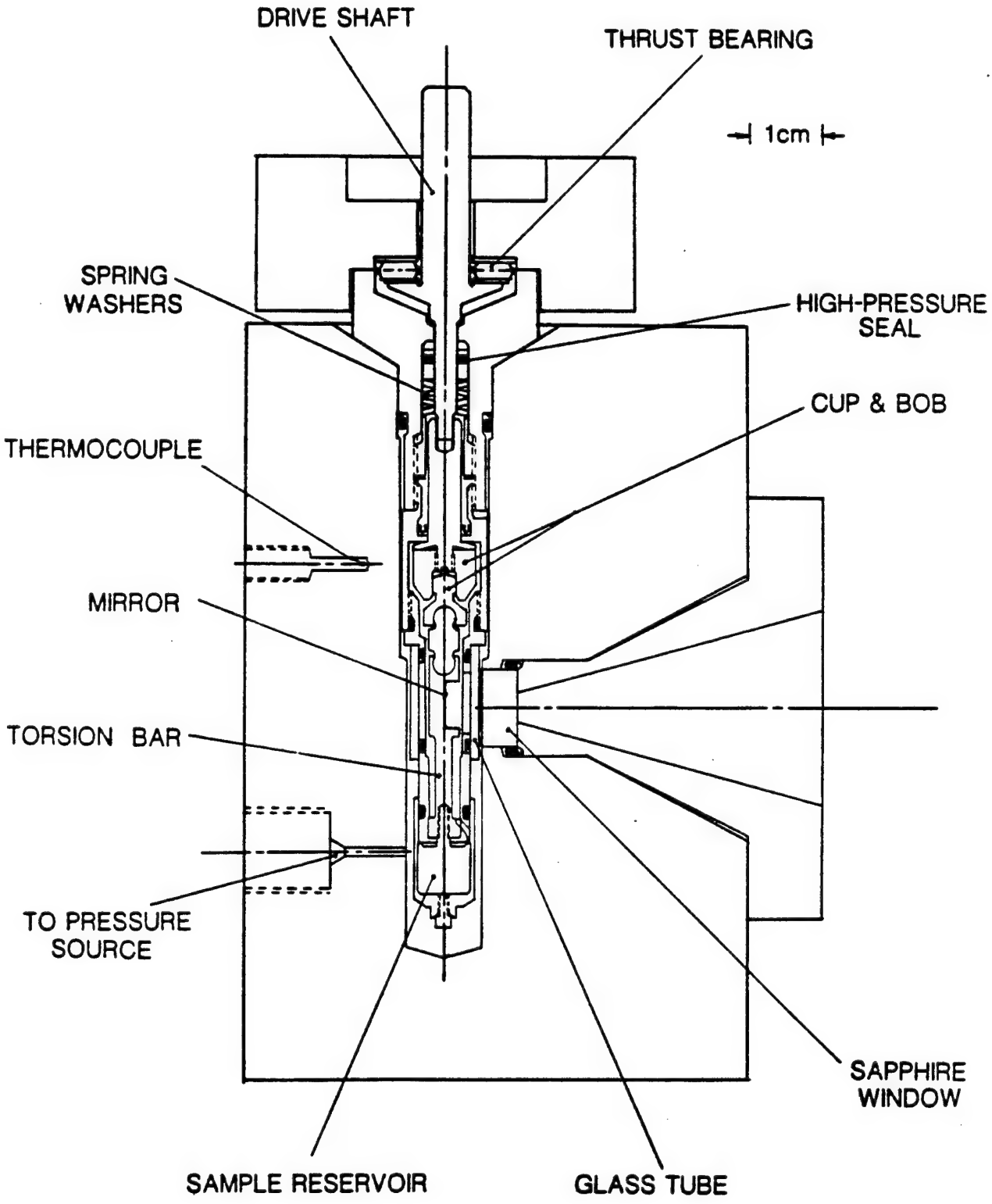

Figure 4 High-Pressure High Shear Stress Viscometer for 600 MPa Pressure.

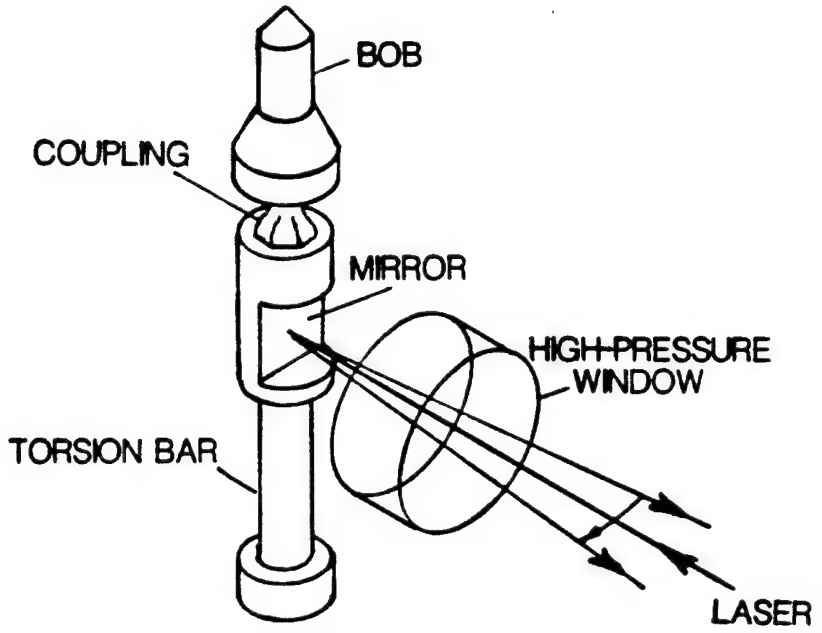

Figure 5 **Torque Transducer Operating Principle for Rheometer Shown in Figure 4**

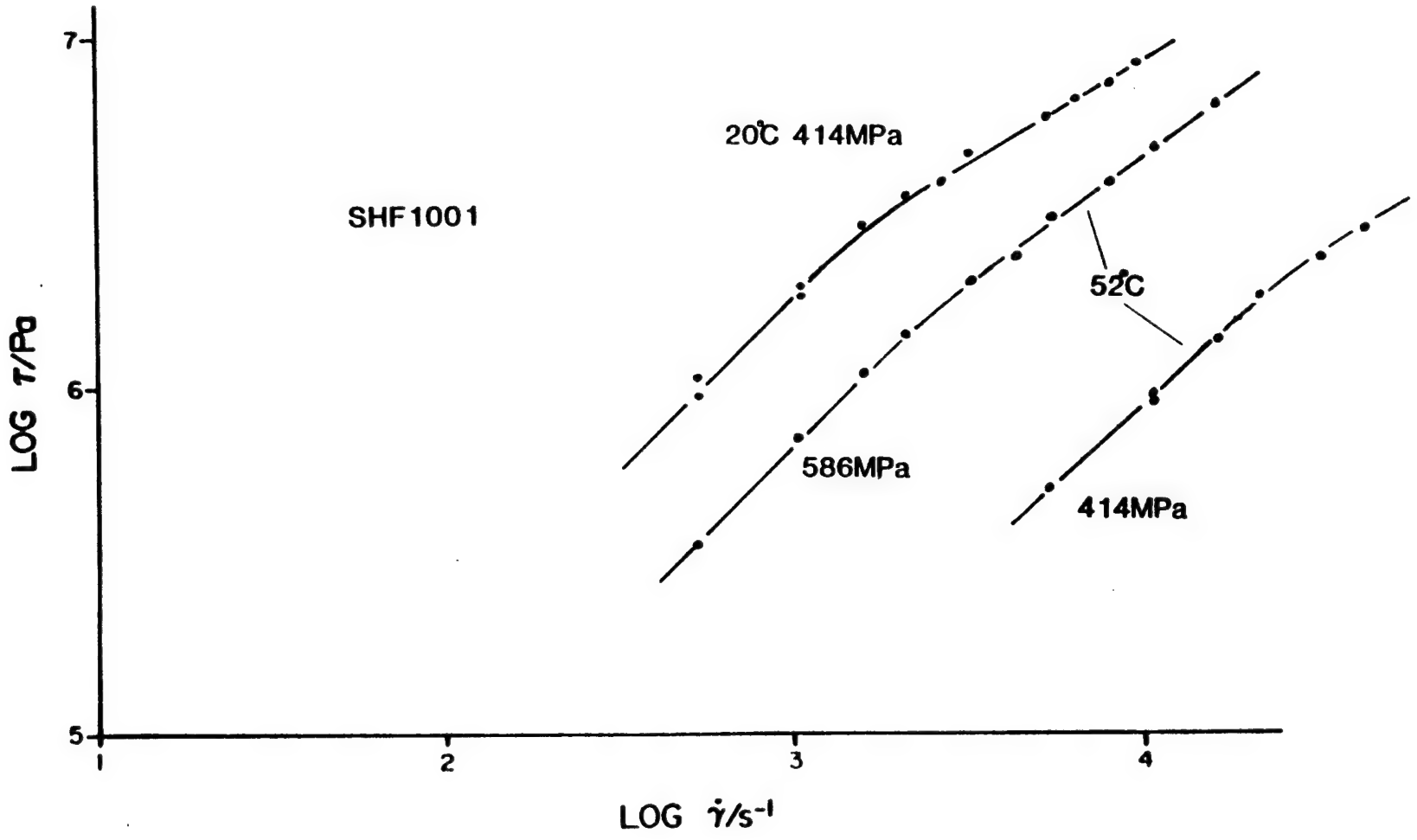

Figure 6 Flow Chart for a Polyalphaolefin.

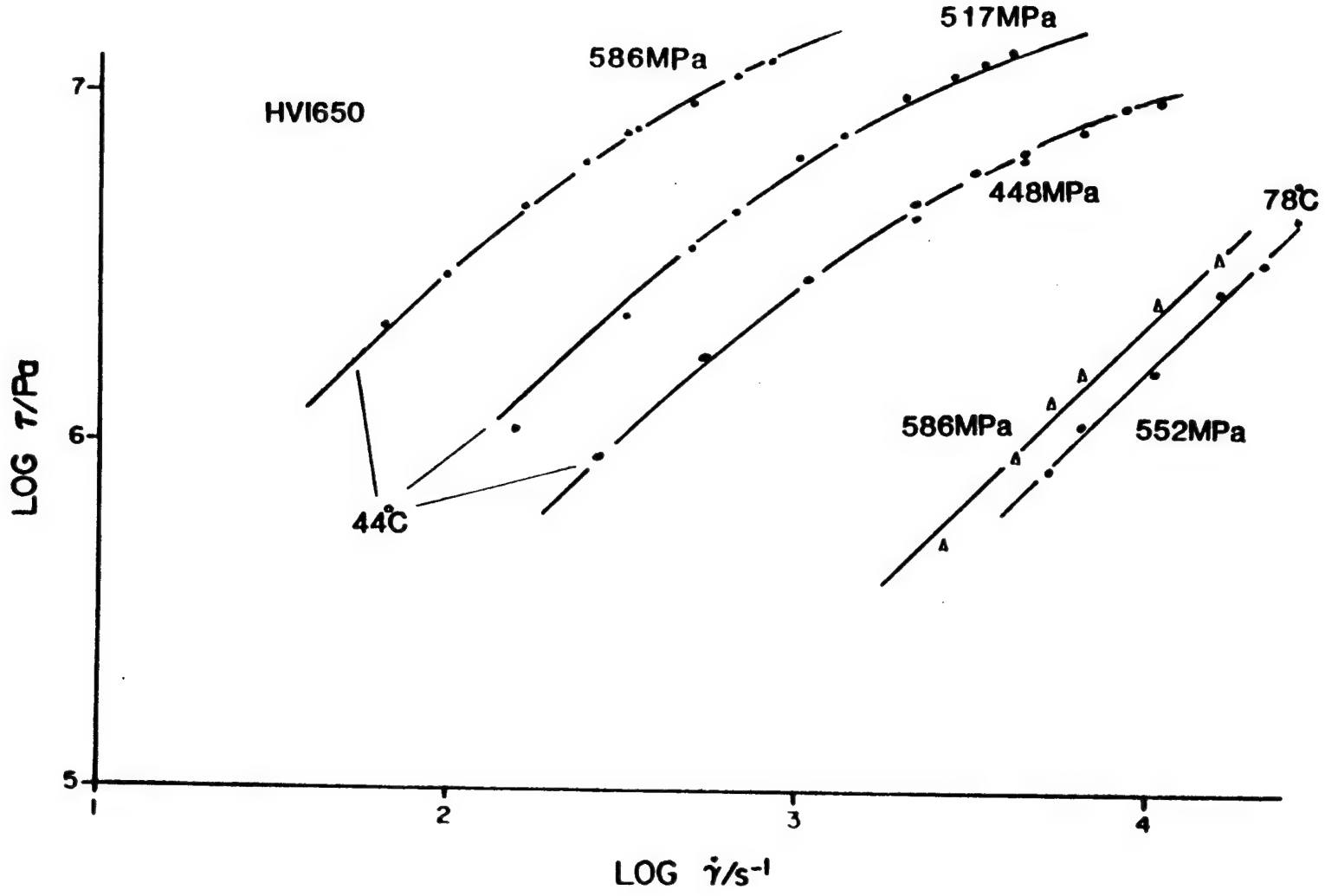

Figure 7 a Flow Chart for HVI 650.

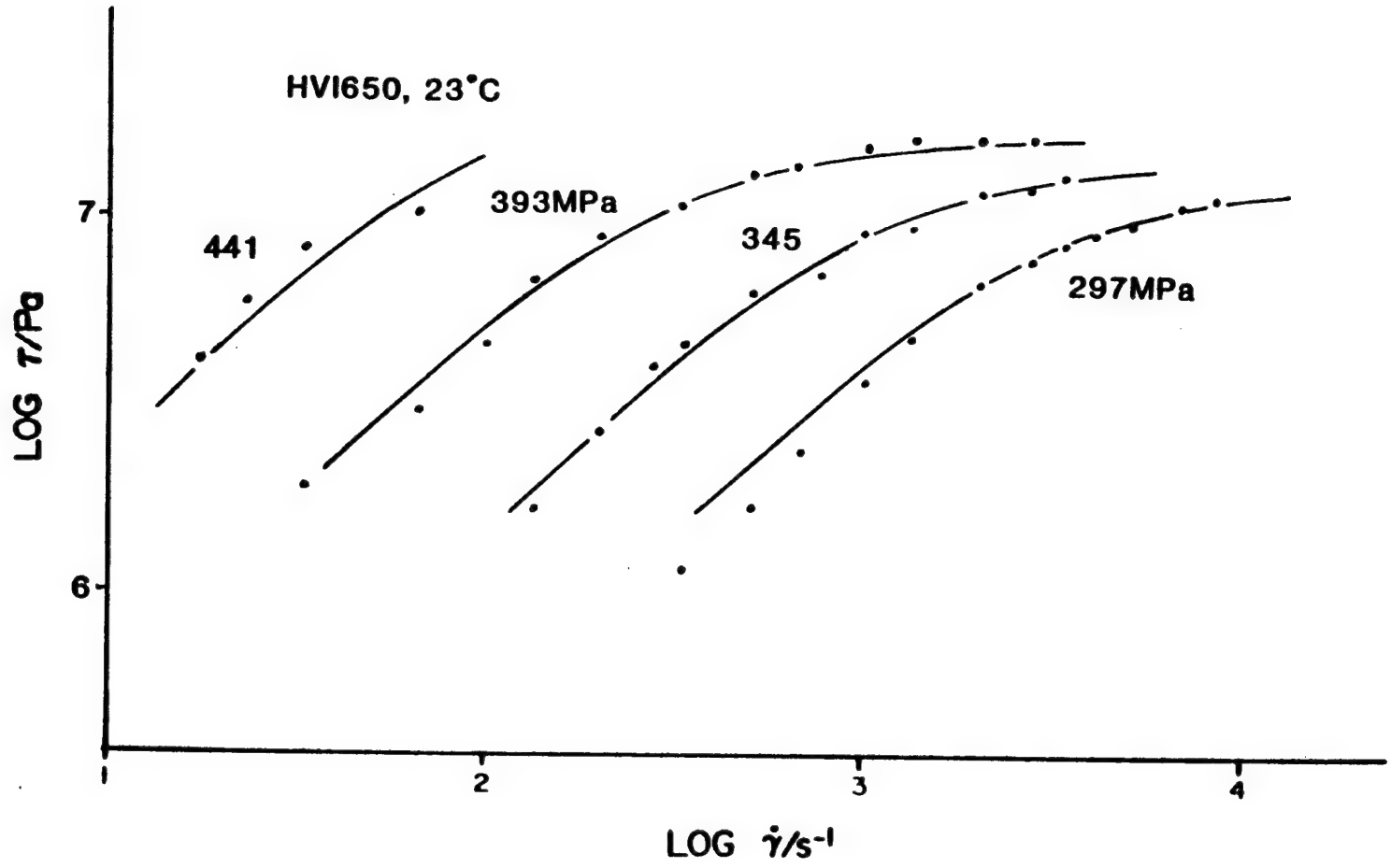

Figure 7b. Flow Chart for HVI 650.

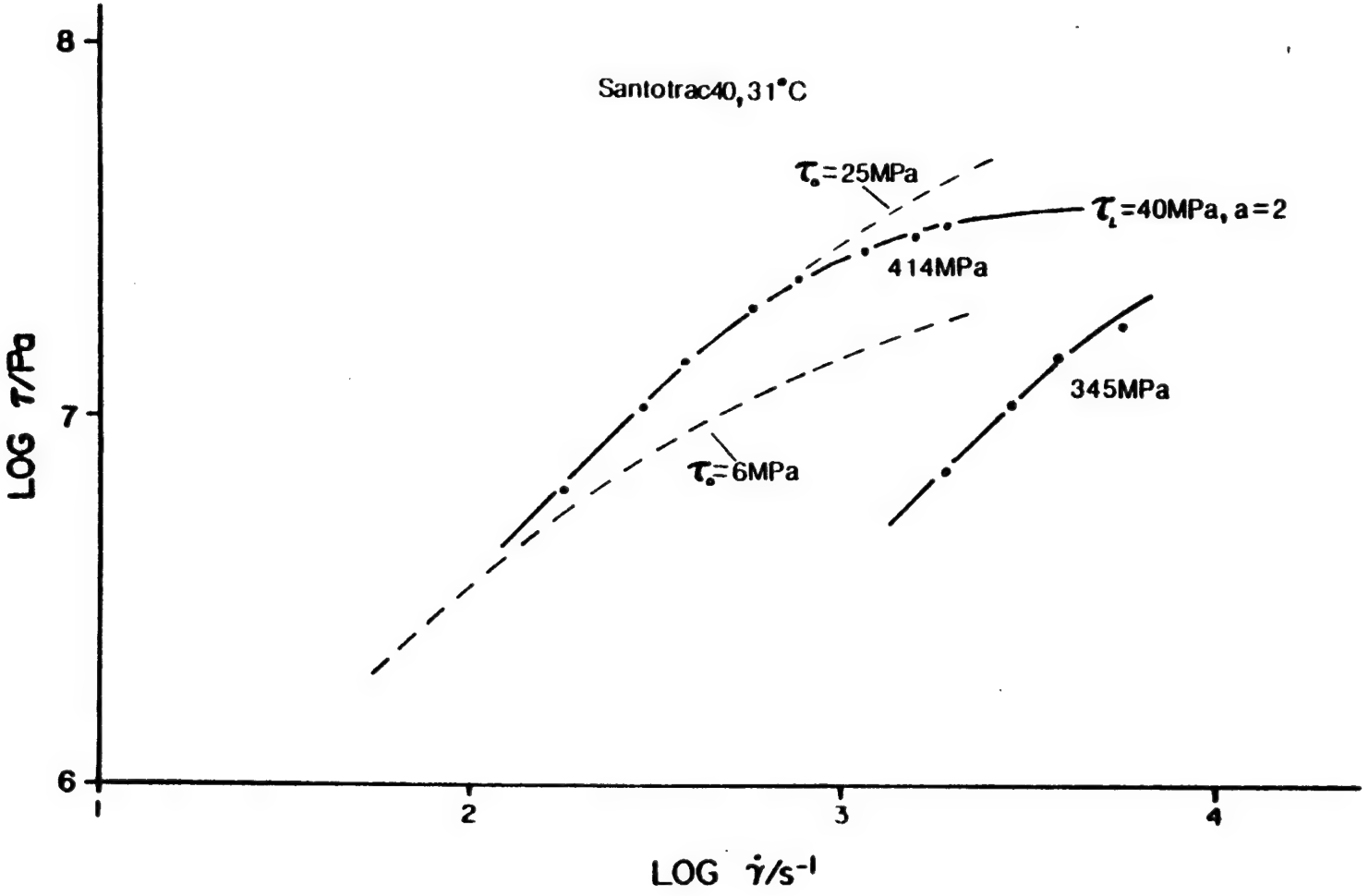

Figure 8. Flow Chart for Santotrac 40

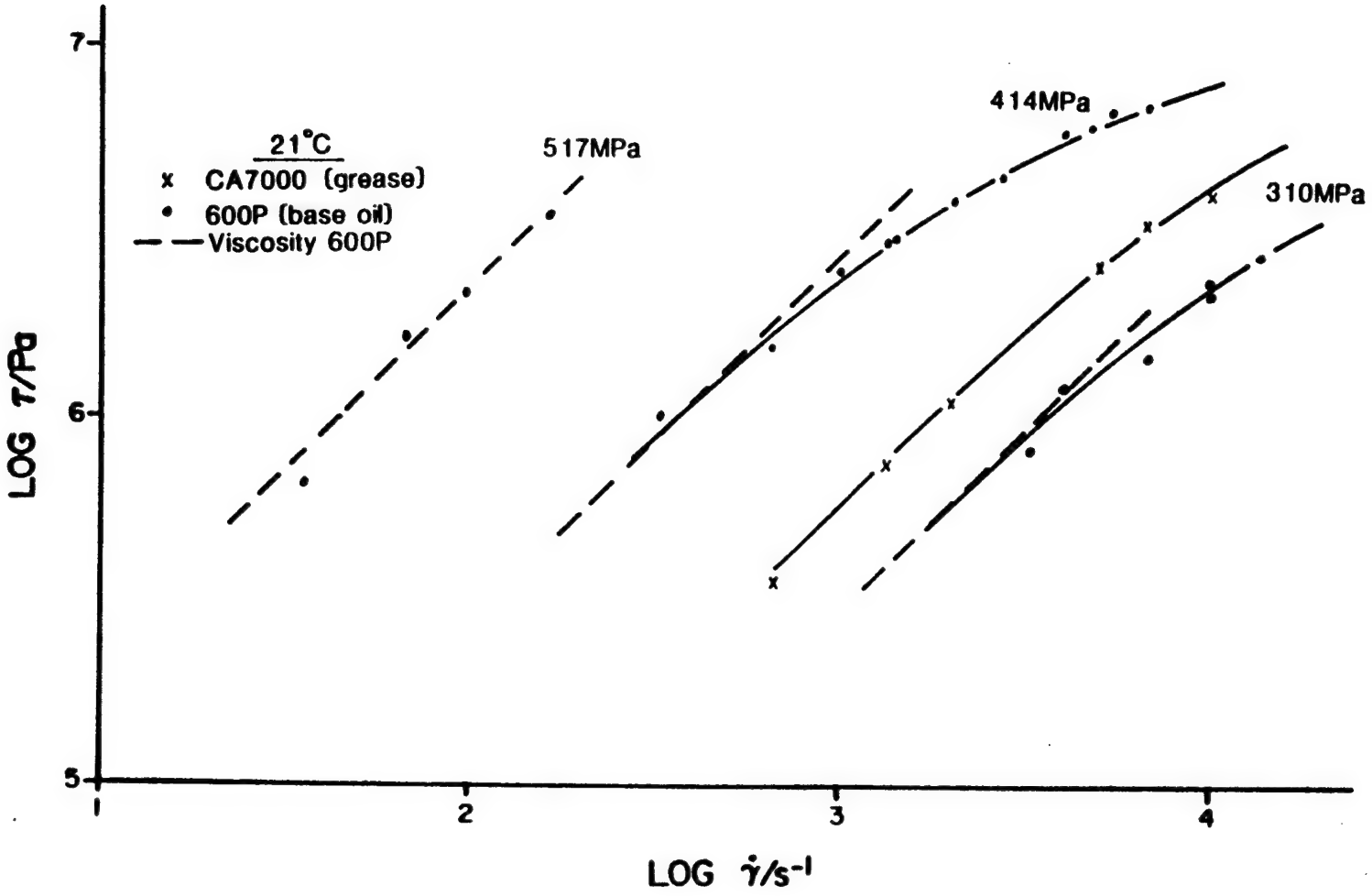

Figure 9 Flow Chart for Grease and Base Oil.

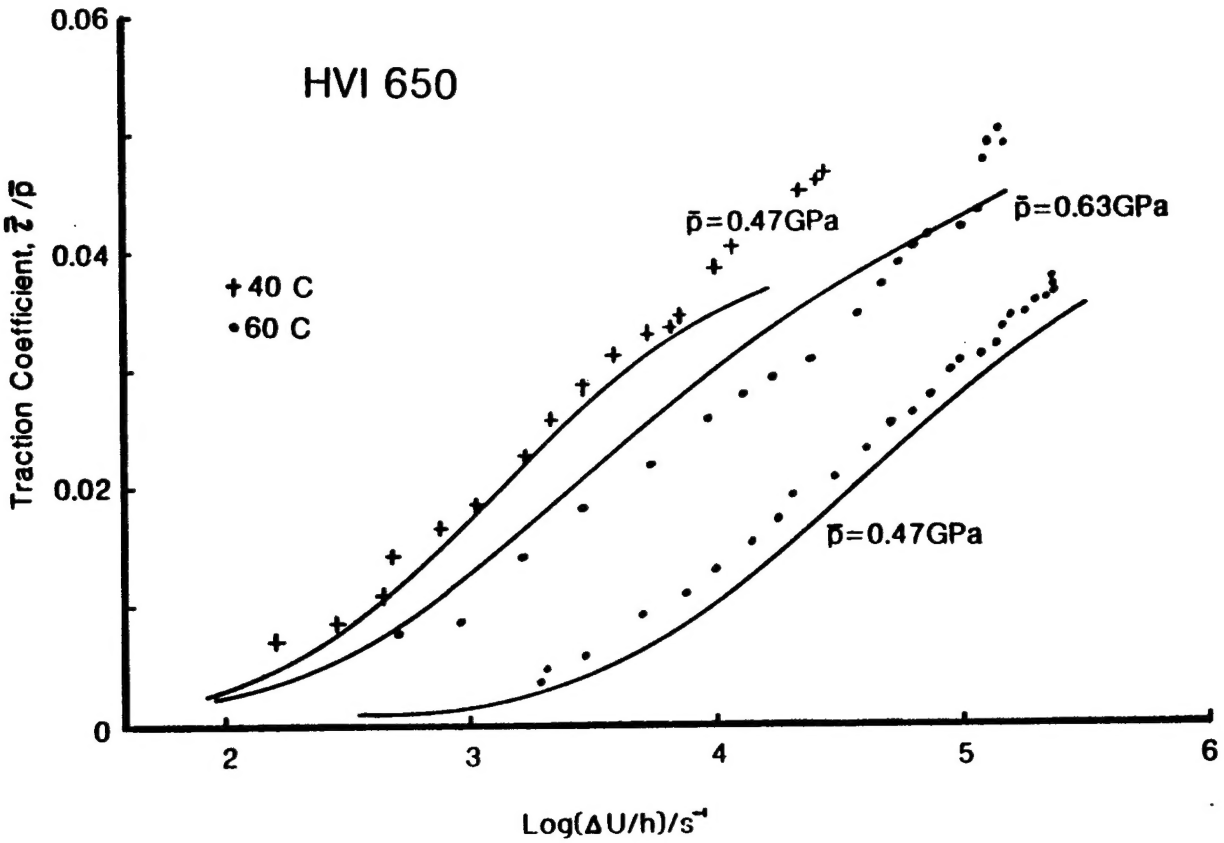

Figure 10. Measured and Predicted Traction Curves for HVI 650.

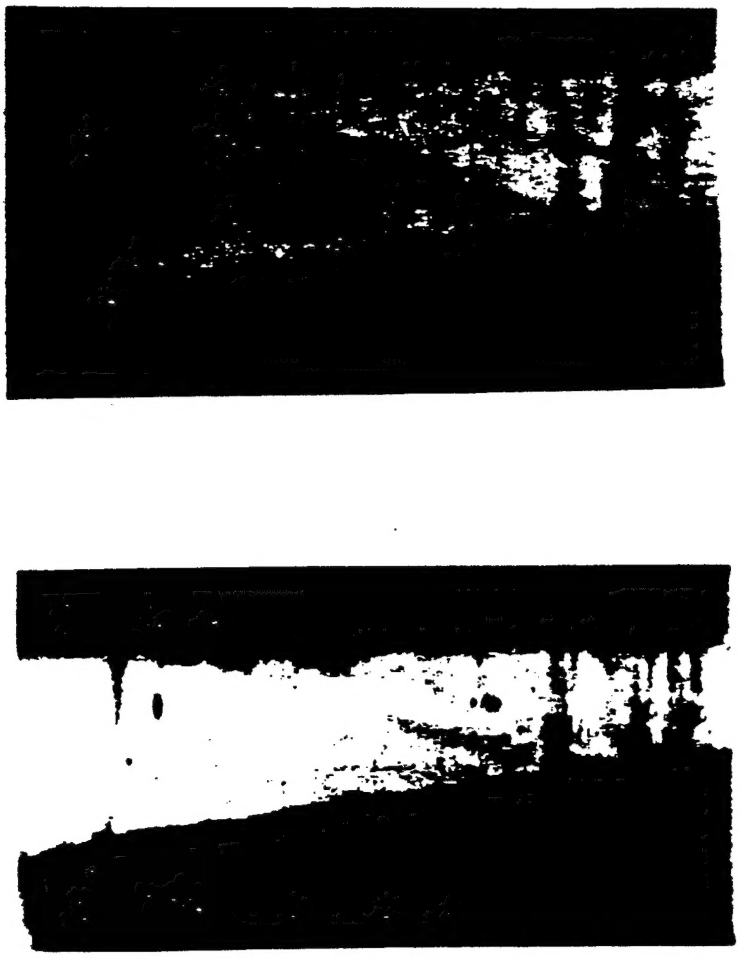

5P4E. 138 MPa, 5°C

Figure 11. Mechanical Shear Bands between Converging Plates with Sliding. Lower Tilted Surface is Stationary.

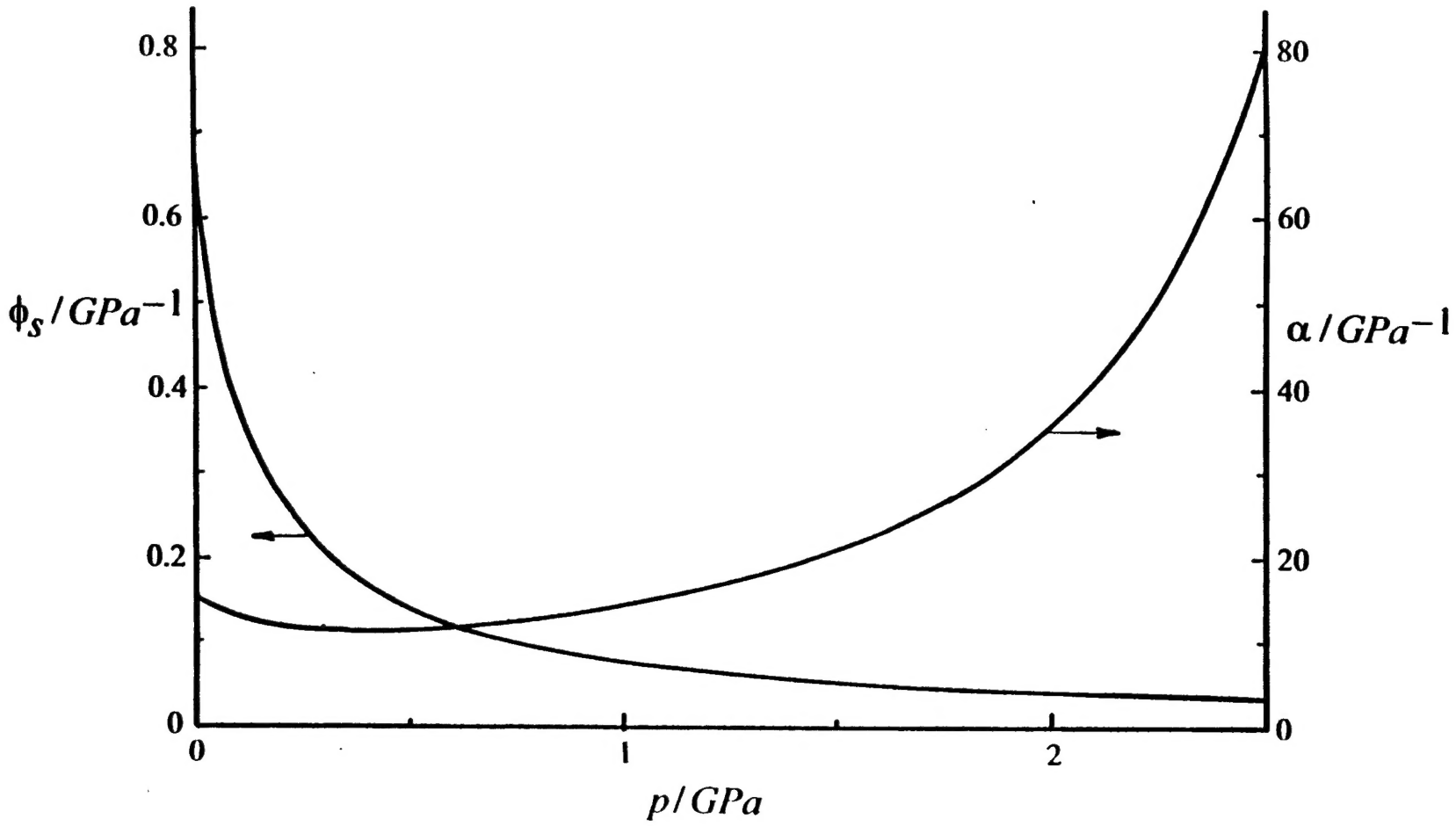

Figure 12. **The variation of compressibility and pressure viscosity coefficient with pressure.**

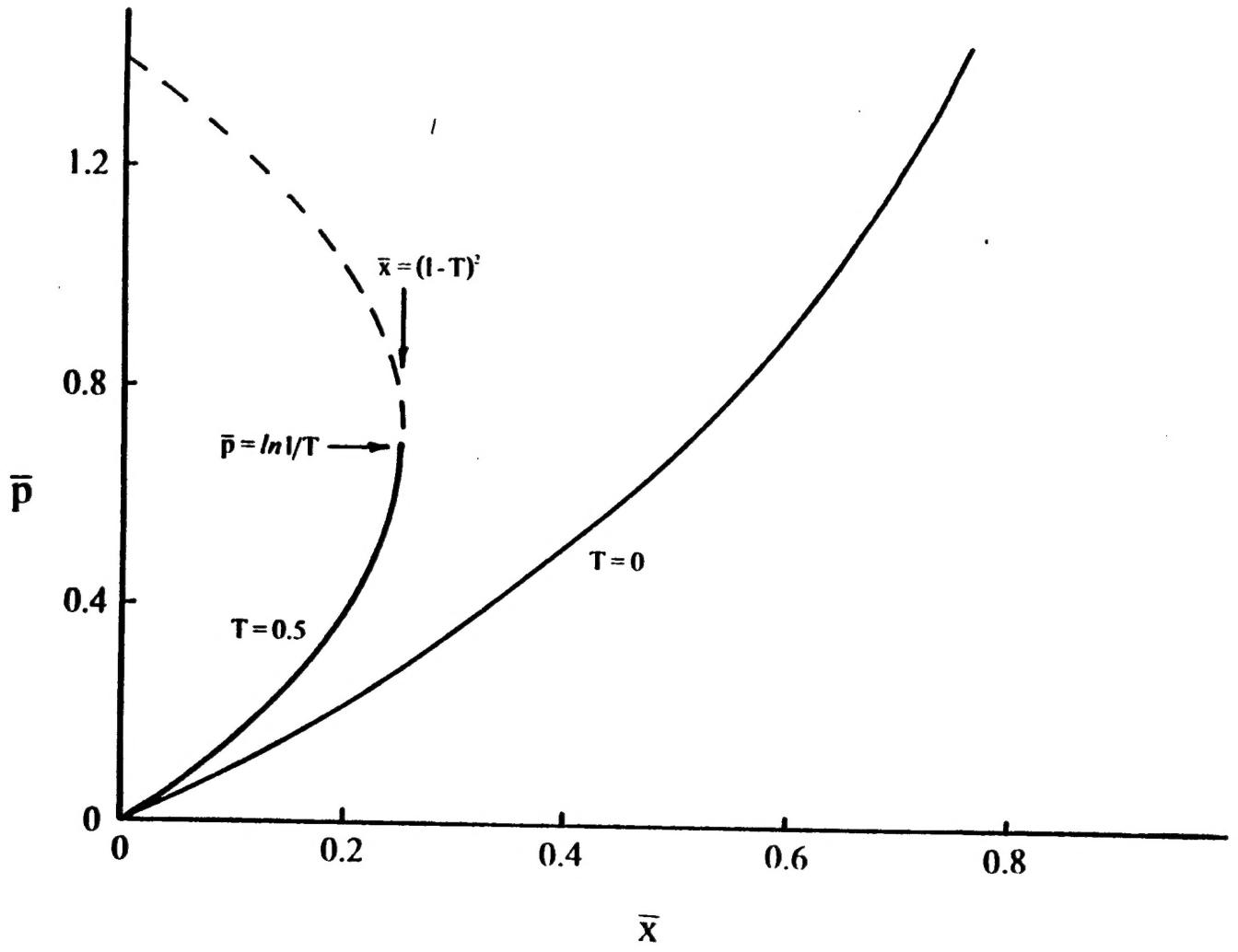

Figure 13. **Pressure along a constant z plane assuming** $w \geq 0$